Assessing the Accuracy of the Damping Models Used in Displacement-Based Seismic Demand Evaluation and Design of Inelastic Structures

Qiang Xue [1)]

1) *Civil and Hydraulic Engineering Research Center, Sinotech Engineering Consultants Inc., Taipei, Taiwan 105, R.O.C.*

ABSTRACT

The response of inelastic structures can be evaluated by using either the elastic response evaluation method or the inelastic evaluation method. The former considers the use of an equivalent linear system represented by an equivalent elastic spectrum, which is associated with the effective damping model, to estimate the nonlinear response. The latter employs the inelastic spectrum directly. In this paper, a non-iterative capacity-spectrum method regardless of the type of spectrum is proposed to estimate the displacement response. The accuracy of the effective damping model is assessed by the error in the displacement response comparing with that obtained using the inelastic evaluation method.

INTRODUCTION

The idea of using the effective damping model has been widely used in the displacement-based seismic demand evaluation and design. Gulkan and Sozen [1] developed the concept of substitute structure to estimate the nonlinear structural response through an equivalent elastic model assuming a linear behavior and effective viscous damping. This idea has been adopted recently by Kowalsky, *et al.* [2] for a direct displacement design of SDOF reinforced concrete structures and by Priestley, *et al.* [3] for both SDOF and MDOF bridges and buildings starting from a target peak displacement. The capacity spectrum method is a simplified method to estimate the inelastic response of structures without performing the computationally ineffective time history analysis. It has been subjected to a lot of studies recently due to the development of performance-based earthquake engineering [4]. This method uses the intersection of the capacity curve from a pushover analysis and a response spectrum (demand) curve under ground shaking to estimate the maximum displacement. Literatures on such method have been documented in ATC-40 [5] and by Freeman [6], Reinhorn [7] Fajfar [8], Chopra & Goel [9] and other researchers. The capacity curve is obtained through the monotonic nonlinear pushover analysis, converted to A-D format via the natural mode shape of the structure, the modal mass coefficient and participation factors. The demand curve accounting for the nonlinear inelastic behavior of a structural system can be represented either by an equivalent elastic response spectrum [5,6] or an inelastic response spectrum [7~9]. The former is associated with effective viscous damping ξ_{eff} equivalent to the non-linear response. That is, the elastic demand curve, determined from an elastic spectral analysis, is modified to account for the hysteretic energy dissipation. The latter is directly constructed based on relations between reduction factors and ductility. Although Chopra and Goel [9] found that ATC-40 [5] procedures A and B using the damping model might result in failure of convergence or give divergent results from the exact solutions even if they are converged. However, the author believes that the reason that causes the failure of convergence is the selection of an unreasonable start point for each iteration in the prescribed procedure and the divergent results comes from the effective damping model used [10].

From the discussions above, the effective damping model plays an important role in giving an accurate result in the direct displacement-based design method or in the displacement demand estimation. The significance of the approximate linearization method incorporating the effective damping model has been introduced by Iwan and Gates [11]. In their study, a technique is presented for estimating the accuracy of different approximate methods available at that time. This paper presents an alternative method to investigate the accuracy of the damping model. The effectiveness of the proposed method is finally demonstrated though its implementation into several damping models.

In the development of performance-based earthquake engineering, which stresses the inelastic behavior of structural systems under severe earthquake ground motions, displacement rather than force has been recognized as the most suitable and direct performance or damage indicator [12]. In this paper, the accuracy of the damping model is consistent with the accuracy of the displacement it gives comparing with that obtained using an inelastic spectrum in the capacity-spectrum method. In this paper, the Newmark-Hall [13] inelastic spectrum is adopted.

A NON-ITERATIVE CAPACITY-SPECTRUM METHOD

The iterative capacity-spectrum procedure has been discussed in detail in ATC-40 [5] and by Freeman [6]. Such iterative procedures may be unnecessary in determining the seismic response when using the numerical version of inelastic response spectrum [9] or other methods. In this section, a non-iterative procedure regardless of the type of response spectrum (equivalent elastic or inelastic) is formulated.

Formulation of the Diagram Reduction Factors

Based on Newmark and Hall [13] studies, response spectra can be enveloped by a plot with three distinct ranges: a constant peak spectral acceleration (PSA), constant peak spectral velocity (PSV) and constant peak spectral displacement (PSD). In the capacity-spectrum method, the response spectrum is plotted in spectral acceleration versus spectral displacement (A-D) format. This A-D format is termed ADRS by Maheney, *et al.* [14] or capacity-demand-diagram by Chopra and Goel [9].

For inelastic systems, the constant-ductility design diagram (A-D format) can be established by both the two procedures shown in Fig.1. One is to multiply the elastic design spectrum (A-T format) by appropriate spectrum reduction factors (SR_A, SR_V and SR_D) to obtain the inelastic [13] or equivalent elastic [5] design spectrum (A-T format) and then transform to A-D format [9]. The other is to transform the elastic design spectrum (A-T format) to elastic design diagram (A-D format) first and then multiply by the corresponding diagram reduction factors (SR_{AD}, SR_{VD} and SR_{DD}). The subscriptions A, V and D indicate the constant spectral acceleration, velocity and displacement range. Notice that in building code or guidelines such as ATC-40, spectrum reductions are suggested only in the constant acceleration and velocity ranges. It is easy to find that the diagram reduction factors and spectral reduction factors are identical for the (equivalent) elastic system (Figs. 1 and 2). Our purpose is to formulate the diagram reduction factors for the inelastic system. The detail formulation can be found in Xue [15] and is briefly summarized here.

$$SR_{AD} = SR_A \tag{1}$$

$$SR_{VD} = \sqrt{\mu} \times SR_V \tag{2}$$

$$SR_{DD} = \mu \times SR_D \tag{3}$$

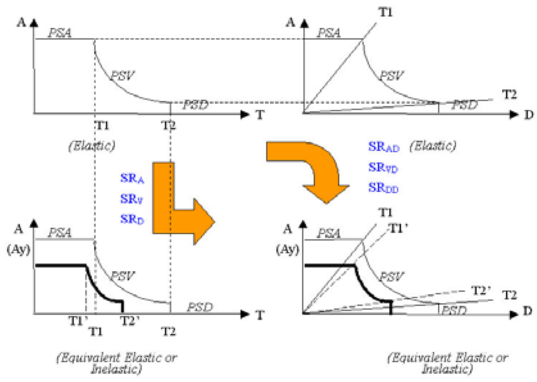

Fig. 1 Spectrum and diagram reduction factors

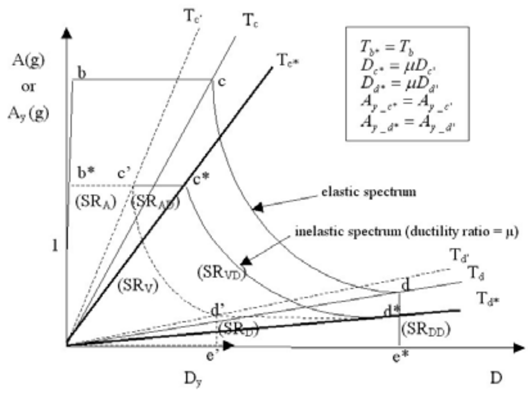

Fig. 2 Equivalent elastic and inelastic design diagram

Thus, the inelastic design diagram and the equivalent elastic design diagram can be constructed in the same way (Fig. 2) by using the diagram reduction factor (Eqs. (1) ~ (3)) for the inelastic design diagram and by the spectrum reduction factor, which will be discussed later, for the equivalent elastic spectra.

The Non-Iterative Procedure

In the capacity-spectrum procedure, the capacity curve of an inelastic system is usually obtained from a non-linear static pushover analysis and represented by a bi-linear force-displacement model (base-shear versus top displacement for

MDOF systems) and also transformed to A-D format (Fig. 3(a)). In Fig. 3(a), the post-yield stiffness ratio is r. The yielding point is denoted as (A_{ye}, D_{ye}). The displacement ductility ratio at the final performance point P is μ_P. Thus, the displacement at the performance point is given by

$$D_P = \mu_P \times D_{ye} \tag{4}$$

And the spectral acceleration at the performance point

$$A_P = A_{ye}(r\,\mu_P - r + 1) \tag{5}$$

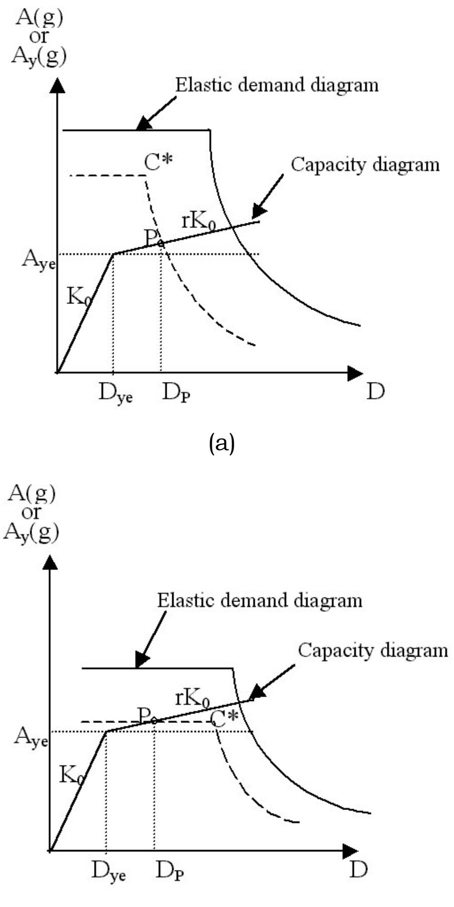

Fig. 3 Performance point from a non-iterative capacity-spectrum method

The demand diagram for the inelastic system passing the performance point is assumed constructed directly from the elastic design diagram with the diagram reduction factors SR_{AD}, SR_{VD}, and SR_{DD} as discussed above. We have,

$$A_P = SR_{VD} \times \left(\frac{2\pi}{T_P}\right) \times PSV \tag{6}$$

$$D_P = \left(\frac{T_P}{2\pi}\right)^2 \times SR_{VD} \times \left(\frac{2\pi}{T_P}\right) \times PSV$$
$$= \left(\frac{T_P}{2\pi}\right) \times SR_{VD} \times PSV \tag{7}$$

From Eqs. (4) and (7), the ductility ratio at the performance point is derived as

$$\mu_P = \left(\frac{T_P}{2\pi}\right) \times SR_{VD} \times \frac{PSV}{D_{ye}} \tag{8}$$

From Eqs. (5) and (6),

$$T_P = \frac{SR_{VD} \times 2\pi \times PSV}{A_{ye} \times (r\,\mu_P - r + 1)} \tag{9}$$

Substituting Eq. (9) to Eq. (8) leads to

$$\mu_P = \frac{SR_{VD}^2 \times PSV^2}{D_{ye} \times A_{ye} \times (r\,\mu_P - r + 1)} \tag{10}$$

For an elasto-plastic system (r = 0) under the same earthquake ground motion, μ_P is proportional to SR_{VD}^2. Thus, the displacement demand D_P is proportional to SR_{VD}^2 (Eq. (4)).

For the case shown in Fig. 3(b),

$$A_P = PSA \times SR_{AD} \tag{11}$$

and

$$A_P = A_{ye} \times (r\,\mu_P - r + 1) \tag{12}$$

For the same system under the same earthquake ground motion using different approaches, μ_p, thus D_p is proportional to SR_{AD}.

Equations. (1) and (2) indicate that SR_{AD} and SR_{VD}^2 are associated with the ductility ratio and/or the spectrum reduction factors SR_A and SR_V, respectively. As will be discussed later, these factors are associated with the damping model and the ductility ratio, therefore, the error in the estimated displacement demand can be characterized by the damping model.

THE SPECTRUM REDUCTION FACTORS

In the capacity-spectrum method using the equivalent elastic spectrum [5], the spectrum reduction factors (SR_A, SR_V and SR_D), that are identical to the diagram reduction factors as discussed above, are based on mean spectrum amplification factors presented by Newmark and Hall [13].

$$SR_A = \frac{3.21 - 0.68 \ln(\zeta_{eff})}{2.12} \quad (13)$$

$$SR_V = \frac{2.31 - 0.41 \ln(\zeta_{eff})}{1.65} \quad (14)$$

where "2.12" and "1.65" are the corresponding amplification factors with respect to the 5% damped elastic design spectrum.

On the other hand, the Newmark and Hall [13] inelastic spectrum is established by multiplying the 5% damped elastic design spectrum by the spectrum reduction factors

$$SR_A = \frac{1}{\sqrt{2\mu - 1}} \quad (15)$$

$$SR_V = SR_D = \frac{1}{\mu} \quad (16)$$

THE DAMPING MODELS

5 damping models are considered in this paper and are briefly presented in this section.

1. The ATC-40 [5] damping model is based on that the energy dissipated by the inelastic structure is equal to that dissipated by an equivalent viscous system in a single cycle of motion [16]. The effective damping ζ_{eff} is composed of the equivalent viscous damping ζ_{eq} and the viscous damping inherent in the structure (e.g., 5%).

$$\zeta_{eff} = \zeta_0 + \zeta_{eq} = 5 + \kappa \frac{2(\mu - 1)(1 - r)}{\pi \mu (1 + r\mu - r)} \quad \text{(in percent)} \quad (17)$$

where μ and r are the ductility ratio and the post-yielding stiffness ratio, respectively. κ is a damping modification factor associated with the hysteresis behavior type [5] of the structure.

2. The WJE [17] damping model is based on that the maximum displacement determined from the elastic design spectrum is equal to that obtained from the inelastic design spectrum (Table 1).

Table 1 The WJE damping model

μ	1.0	1.25	1.5	2.0	3.0	4.0
ζ_{eff} (%) (based on median + 1-standard-deviation spectrum)	5.0	7.5	10	14	21	26
ζ_{eff} (%) (based on median spectrum)	5.0	8.5	12	16	26	35

3. The damping model used by Kowalsky, *et al.* [2] is based on the laboratory test results and curve fitting.

$$\zeta_{\text{eff}} = \zeta_0 + \zeta_{\text{eq}} = 0.05 + 0.39372\left[1 - \frac{1}{\sqrt{\mu}}\right] \tag{18}$$

4. The damping model used by Preistley, *et al.* [3] is based on Takeda hysteresis model.

$$\zeta_{\text{eff}} = \zeta_0 + \zeta_{\text{eq}} = 0.05 + \frac{1 - \mu^n\left(\frac{1-r}{\mu} + r\right)}{\pi} \tag{19}$$

where the stiffness degradation factor n equals to 0 for steel structures and 0.5 for RC structures.

5. The damping model used by Reinhorn [7] and Kunnath, *et al.* [18] is based on the average stiffness and energy method presented by Iwan and Gates [11].

$$\zeta_{eff} = \left(\frac{3}{2\pi\mu^2}\right) \cdot \frac{\pi\zeta_0\left[(1-r)\left(\mu^2 - \frac{1}{3}\right) + \frac{2}{3} r\mu^3\right] + 2(1-r)(\mu-1)^2}{(1-r)(1+\ln\mu) + r\mu} \tag{20}$$

where ζ_0 is the inherent viscous damping (e.g., 5%).

ASSESSING THE ACCURACY OF THE DAMPING MODELS

According to the above descriptions, the displacement response is proportional either to SR_{VD}^2 (Fig. 3a) or SR_{AD} (Fig. 3b). SR_{VD}^2 and SR_{AD} are associated with the spectral reduction factors SR_V and SR_A through Eqs. (1) and (2), which are valid for both inelastic and equivalent elastic spectra. If the Newmark-Hall inelastic spectrum is used as the demand curve, SR_V and SR_A are evaluated using Eqs. (15) and (16). If an equivalent elastic spectrum is employed as the demand curve, SR_V and SR_A are calculated using Eqs. (13) and (14) with the effective damping ζ_{eff} described in the last section. Therefore, the effectiveness of the damping model is characterized by the error in the estimated displacement response, i.e., the error in SR_{VD}^2 or SR_{AD}, comparing with that by using the inelastic spectrum. The detail calculated results are shown in Tables 2~5 and Figs. 4, 5. From these tables and figures, the error produced by using the WJE [17] model is within 10% since it is based on the factors mapping from the inelastic spectrum. Among others, for structures with ductility ratio less than 4, the damping model based on the average stiffness and energy method presented by Iwan and Gates [11] gives the most accurate results. For structural ductility ratio greater than 4, the ATC-40 [5] damping model with hysteresis behavior type A produces the smallest error.

Table 2 The diagram reduction factor SR_{VD} estimated using various models

μ	SR_{VD} (Newmark-Hall inelastic spectrum	ATC-40 (type A)		ATC-40 (type B)		ATC-40 (type C)		WJE		Kowalsky, *et al.*		Priestley, *et al.*		Reinhorn	
		ζ_{eff} (%)	SR_{VD}	ζ_{eff} (%)	SR_{VD}	ζ_{eff} (%)	SR_{VD}	ζ_{eff} (%)	SR_{VD}	ζ_{eff} (%)	SR_{VD}	ζ_{eff} (%)	SR_{VD}	ζ_{eff} (%)	SR_{VD}
1	1.00	5.00	1.00	5.00	1.00	5.00	1.00	5.00	1.00	5.00	1.00	5.00	1.00	5.00	1.00
1.25	0.89	18.10	0.68	13.00	0.76	9.00	0.85	8.50	0.87	9.16	0.85	8.36	0.87	7.95	0.88
1.5	0.82	25.38	0.60	18.00	0.68	11.00	0.80	12.00	0.78	12.22	0.78	10.84	0.81	12.10	0.78
2	0.71	32.87	0.53	25.00	0.60	16.00	0.71	16.00	0.71	16.53	0.70	14.32	0.74	18.16	0.68
3	0.58	38.55	0.49	29.00	0.56	19.00	0.67	26.00	0.59	21.64	0.64	18.45	0.68	23.66	0.61
4	0.50	40.00	0.48	29.00	0.56	20.00	0.66	35.00	0.52	24.69	0.60	20.92	0.64	25.59	0.59
6	0.41	40.00	0.48	29.00	0.56	20.00	0.66			28.30	0.57	23.84	0.61	26.42	0.59
8	0.35	40.00	0.48	29.00	0.56	20.00	0.66			30.45	0.55	25.58	0.59	26.16	0.59

Table 3 Error in the estimated displacement response characterized by that in SR_{VD}^2

μ	Error in SR_{VD}^2 (%)						
	ATC-40 (type A)	ATC-40 (type B)	ATC-40 (type C)	WJE	Kowalsky *et al.*	Priestley *et al.*	Reinhorn
1	0	0	0	0	0	0	0
1.25	– 42	– 27	– 9	– 6	– 10	– 5	– 2
1.5	– 47	– 30	– 3	– 8	– 9	– 2	– 9
2	– 43	– 28	1	1	– 1	9	– 8
3	– 27	– 5	34	5	21	37	13
4	– 7	27	72	7	46	66	41
6	40	90	158		95	125	106
8	87	154	244		143	183	177

Table 4 The diagram reduction factor SR_{AD} estimated using various models

μ	SR_{AD} (Newmark-Hall inelastic spectrum)	ATC-40 (type A)		ATC-40 (type B)		ATC-40 (type C)		WJE		Kowalsky, *et al.*		Priestley, *et al.*		Reinhorn	
		ζ_{eff} (%)	SR_{AD}	ζ_{eff} (%)	SR_{AD}	ζ_{eff} (%)	SR_{AD}	ζ_{eff} (%)	SR_{AD}	ζ_{eff} (%)	SR_{AD}	ζ_{eff} (%)	SR_{AD}	ζ_{eff} (%)	SR_{AD}
1	1.00	5.00	1.00	5.00	1.00	5.00	1.00	5.00	1.00	5.00	1.00	5.00	1.00	5.00	1.00
1.25	0.82	18.10	0.59	13.00	0.69	9.00	0.81	8.50	0.83	9.16	0.80	8.36	0.83	7.95	0.85
1.5	0.71	25.38	0.48	18.00	0.59	11.00	0.75	12.00	0.72	12.22	0.71	10.84	0.75	12.10	0.71
2	0.58	32.87	0.39	25.00	0.48	16.00	0.62	16.00	0.62	16.53	0.61	14.32	0.66	18.16	0.58
3	0.45	38.55	0.34	29.00	0.43	19.00	0.57	26.00	0.47	21.64	0.53	18.45	0.58	23.66	0.50
4	0.38	40.00	0.33	29.00	0.43	20.00	0.55	35.00	0.37	24.69	0.49	20.92	0.54	25.59	0.47
6	0.30	40.00	0.33	29.00	0.43	20.00	0.55			28.30	0.44	23.84	0.50	26.42	0.46
8	0.26	40.00	0.33	29.00	0.43	20.00	0.55			30.45	0.42	25.58	0.47	26.16	0.47

Table 5 Error in the estimated displacement response characterized by that in SR_{AD}

μ	Error in SR_{AD} (%)						
	ATC-40 (type A)	ATC-40 (type B)	ATC-40 (type C)	WJE	Kowalsky, *et al.*	Priestley, *et al.*	Reinhorn
1	0	0	0	0	0	0	0
1.25	– 28	– 15	– 1	1	– 2	2	4
1.5	– 33	– 17	5	1	1	6	1
2	– 32	– 17	8	8	6	14	1
3	– 23	– 3	27	5	18	29	12
4	– 12	15	46	– 1	29	43	25
6	10	44	83		47	65	54
8	28	68	114		62	84	81

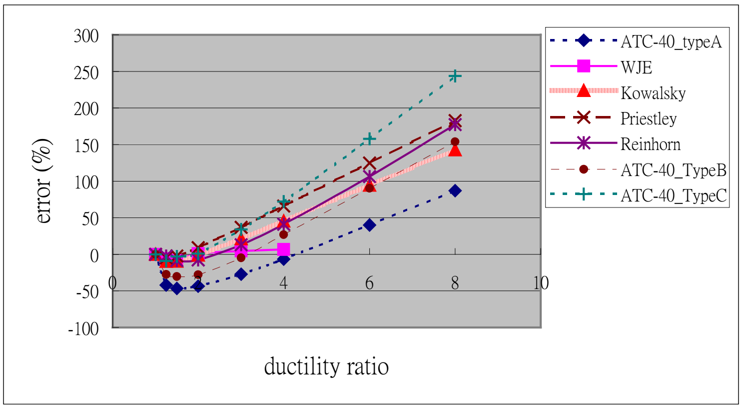

Fig. 4 Error in the estimated displacement response characterized by that in SR_{VD}^2

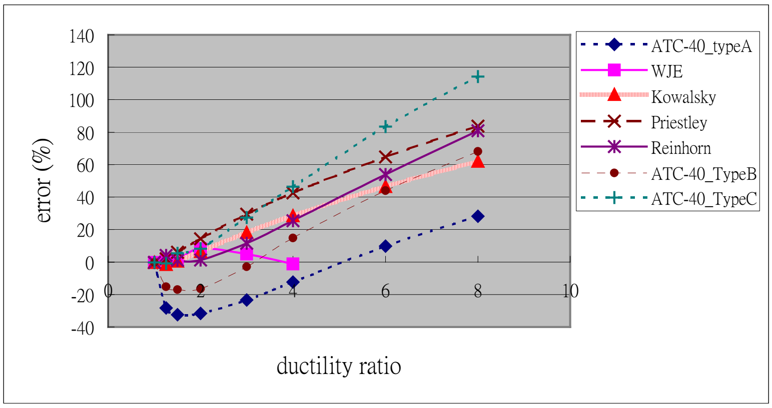

Fig. 5 Error in the estimated displacement response characterized by that in SR_{AD}

CONCLUSIONS

The damping model plays a significant role in the seismic demand estimation and design when using an equivalent linear system to characterize the inelastic structural system. This paper proposes a non-iterative capacity-spectrum method regardless of the type of response spectrum using the so-called diagram reduction factors. Using different algorithms, the displacement response is calculated in the same way through different formulations of the spectrum reduction factors, which are associated with the damping models in the equivalent linear systems. Thus, the accuracy of a damping model is assessed by the error in the displacement response comparing with the displacement obtained through the inelastic spectrum.

REFERENCES

1. Gulkan, P. and Sozen, M. (1974). "Inelastic response of reinforced concrete structures to earthquake motions," *ACI Journal*, Vol. 71, No. 12, pp. 604-610.
2. Kowalsky, M.J., Priestley, M.J.N. and MacRae, G.A. (1994). "Displacement-based design, a methodology for seismic design applied to single degree of freedom reinforced concrete structures," Report No. SSRP-94/16, Structural Systems Research, University of California, San Diego, La Jolla, California.
3. Priestley, M.J.N., Kowalsky, M.J., Ranzo, G. and Benzoni, G. (1996). "Preliminary development of direct displacement-based design for multi-degree of freedom systems," *Proceedings 65th Annual Convention*, SEAOC, Maui, Hawaii.
4. Krawinkler, H. (1999). *Advancing Performance-Based Earthquake Engineering*, http://peer.berkeley.edu/news/1999jan/advance.html.
5. ATC-40 (1996). *Seismic Evaluation and Retrofit of Concrete Buildings,* Vol. 1, Applied Technology Council, Redwood City, California.
6. Freeman, S.A. (1998). "Development and use of capacity spectrum method," *Proceedings of 6th U.S. National Conference on Earthquake Engineering,* Seattle, EERI, Oakland, California.
7. Reinhorn, A.M. (1997). "Inelastic analysis techniques in seismic evaluations," *Seismic Design*

Methodologies for the Next Generation of Codes, Proc. The International Workshop on Seismic Design Methodologies for the Next Generation of Codes, Balkema, Rotterdam, pp. 277–287.

8. Fajfar, P. (1999). "Capacity spectrum method based on inelastic demand spectra," *Earthquake Engineering and Structural Dynamics*, Vol. 28, pp. 979–993.
9. Chopra, A.K. and Goel, R.K. (1999). "Capacity-demand-diagram methods for estimating seismic deformation of inelastic structures: SDF systems," Report No. PEER-1999/02, Pacific Earthquake Engineering Research Center, University of California, Berkeley.
10. Xue, Q. (2001). "A reliable capacity-spectrum method," *8th International Conference on Structural Safety and Reliability*, Newport Beach, California, USA, June 17~21, accepted.
11. Iwan, W.D. and Gates, N.C. (1979). "Estimating earthquake response of simple hysteretic structures," *Journal of the Engineering Mechanics Division*, Vol. 105, No. 3, pp. 391–405.
12. Fajfar, P. and Krawinkler, H. (1997). *Seismic Design Methodologies for the Next Generation of Codes, Proc. The International Workshop on Seismic Design Methodologies for the Next Generation of Codes*, Balkema, Rotterdam.
13. Newmark, N.M. and Hall, W.J. (1982). "Earthquake spectra and design," Earthquake Engineering Research Institute, Berkeley.
14. Mahaney, J.A., Paret, T.F., Kehoe, B.E. and Freeman S.A. (1993). "The capacity spectrum method for evaluating structural response during the Loma Prieta earthquake," *National Earthquake Conference*, Memphis.
15. Xue, Q. (2001). "A direct displacement-based seismic design procedure of inelastic structures," *Engineering Structures*, accepted.
16. Chopra, A.K. (1995). *Dynamics of Structures, Theory and Application to Earthquake Engineering*, Prentice Hall, Englewood Cliffs, New Jersey.
17. WJE (1996). "Seismic dynamic analysis for building," Final manuscription prepared for the U.S. Army Engineering division by Wiss, Janney, Elstner Associates, Inc., Emeryville, California (Unpublished).
18. Kunnath, S.K., Valles-Mattox, R.E. and Reinhorn, A.M. (1996). "Evaluation of seismic damageability of typical R/C building in midwest united states," *11th World Conference on Earthquake Engineering*, Paper No. 1300.